Proceedings of the ASME 2019
Internal Combustion Engine Division Fall Technical Conference
ICEF2019
October 20-23, 2019, Chicago, IL, USA

ICEF2019-7224

DIRECT MEASUREMENT OF AMMONIA STORAGE ON PASSIVE SCR SYSTEMS FOR LEAN GASOLINE NOX REDUCTION USING RADIO FREQUENCY SENSING

Alexander Sappok, Paul Ragaller, Josh Mandelbaum, Luc Lapenta
CTS Corporation, Boston Innovation Office
Malden, MA

Josh Pihl, Vitaly Prikhodko, James Parks II
Oak Ridge National Laboratory
Oak Ridge, TN

ABSTRACT

Lean gasoline engine operation provides clear efficiency benefits relative to conventional stoichiometric combustion approaches. One of the key hurdles to the widespread, practical implementation of lean gasoline combustion remains the challenge of lean NOx control. One of the potential approaches for controlling NOx emission from lean gasoline engines is the so-called passive selective catalytic reduction (SCR) system. In such systems, periods of rich operation generate ammonia over a three-way catalyst (TWC), which is then adsorbed on the downstream SCR and consumed during lean operation. Brief periods of rich operation must occur in response to the depletion of stored ammonia on the SCR, which requires reliable measurements of the SCR ammonia inventory. Presently, lean exhaust system controls rely on a variety of gas sensors mounted up- and downstream of the catalysts, and which only provide an indirect inference of the operation state.

In this study, a radio frequency (RF) sensor was used to provide a direction measurement of the amount of ammonia adsorbed on the SCR in real-time. The RF sensor was calibrated and deployed on a BMW N43B20 4-cylinder lean gasoline engine equipped with a passive SCR system. Brief periods of rich operation performed at lambda values between 0.98 and 0.99 generated the ammonia, subsequently stored on the SCR for consumption during periods of lean operation. The experiments compared real-time measurements of SCR ammonia inventory from the RF sensor with estimates of ammonia coverage derived from exhaust gas composition measurements upstream and downstream of the catalyst. The results showed a high degree of correlation between the RF measurements and SCR ammonia storage inventory, and demonstrated NOx conversion efficiencies above 98%, confirming the feasibility of the concept. Relative to stoichiometric operation, lean-gasoline operation resulted in fuel efficiency gains of up to 10%, which may be further improved through direct feedback control from the RF sensor to optimize lean – rich cycling based on actual, measured SCR ammonia levels.

Keywords: SCR, RF Sensing, Ammonia Storage, Lean Gasoline, NOx Reduction, Passive SCR

NOMENCLATURE

ACEC	Advanced Combustion and Emission Control
CAN	Controller Area Network
DEF	Diesel Exhaust Fluid
DPF	Diesel Particulate Filter
EPA	Environmental Protection Agency
GPF	Gasoline Particulate Filter
LH	Lean Homogenous
LS	Lean Stratified
RF	Radio Frequency
SCR	Selective Catalytic Reduction
TWC	Three-Way Catalyst

INTRODUCTION

In order to meet stringent regulations on tailpipe NOx emissions, especially those introduced in Europe and the United States [1,2], manufacturers have introduced selective catalytic reduction (SCR) systems. SCR technology enables these regulations to be met by reducing exhaust NOx levels to acceptable limits, and thereby enabling optimization of the engine's combustion process.

The NOx reduction process occurs in the catalyst by reacting engine-out NOx with ammonia and other exhaust gas constituents via several chemical pathways. The ammonia is either injected from a secondary source, such as from an on-board diesel exhaust fluid (DEF) tank as in the case of

conventional SCR processes, or via ammonia production over a three-way catalyst (TWC). In conventional SCR processes, ammonia is introduced primarily via injection of urea, or DEF directly into the exhaust upstream of the catalyst. The efficiency of the SCR system depends on several factors, including the optimization of the urea dosing control strategy, which poses significant challenges under transient operating conditions [3]. Improvements to the urea dosing strategy, and thereby ammonia inventory management, enable peak NOx conversion efficiencies resulting in further improvements in powertrain efficiency.

Early urea dosing strategies involved open-loop control methods primarily utilizing look-up tables, which determined the amount of urea required to perform the NOx conversion based on the engine operating conditions. Closed-loop control strategies were introduced to achieve higher NOx conversion and to provide more efficient urea dosing. In order to provide feedback of the ammonia adsorption state, commercial ammonia and NOx sensors are installed upstream and downstream of the catalyst. These sensors, however, only provides an inference of the loading state of the SCR, and these indirect measurements are often confounded due to the cross-sensitivity of current NOx sensors to ammonia [4,5].

Alternative methods, utilizing radio frequencies (RF), enabling direct measurements of the catalyst loading state have also been investigated [6]. These RF sensors rely on measuring changes in the bulk dielectric properties of the material contained within a resonance cavity which is formed by the catalyst housing in the exhaust system. In the case of SCR applications, previous studies have demonstrated the potential to use the RF sensor output as the feedback portion of closed-loop urea dosing control [6-8].

RF sensors have been applied previously to directly measure the soot and ash loading state in diesel particulate filters (DPFs). Responding to dielectric changes within the DPF cavity, due to the increased dielectric loss of the soot build-up, RF sensors are capable of measuring instantaneous soot loads closely correlated with gravimetric measurements [9]. Direct measurements of particulate filter soot load have further been applied to optimize particulate filter regeneration control as part of a closed-loop control strategy [10].

Figure 1 presents an example of an RF sensor used for DPF and SCR measurements. The sensor consists of a control module and one or two RF antennas (probes) used to transmit and receive RF signals with the catalyst housing. The control module enables measurements of signal amplitude and phase (vector measurements) over a broad frequency range. All sensor output is provided over CAN. Although the RF system shown in Figure 1 is used to send, receive, and process the RF measurements, the aftertreatment device (SCR, DPF), and most notably the catalyst housing, is an integral part of the sensing system.

Figure 1. RF sensor for DPF and SCR measurements.

Figure 2 presents a generic catalyst assembly instrumented with two RF antennas. The RF signal is fully-contained within the housing, which forms a microwave resonant cavity. Monitoring changes in the RF signal at resonance enables direct measurement of the chemical or physical processes occurring within the housing, which are manifest as a change in the system's dielectric properties. Details of the technique, including measurement fundamentals have been described in previous publications [7,9-11].

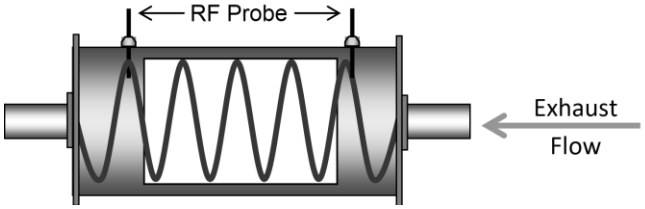

Figure 2. RF antennas installed on catalyst.

Extensive previous research has been performed to characterize the behavior of RF sensors during real operation and to explore the potential for their use in control and diagnostics applications. An early study demonstrated the potential to monitor the soot accumulation and oxidation processes occurring on DPFs during loading and regeneration cycles [12]. Additional studies have applied RF sensors to provide feedback for filter management and perform diagnostic monitoring functions when utilized to measure soot and ash [13], or when sampled rapidly [14].

This study utilizes the RF sensing platform described so far to measuring the state of the catalyst in passive NOx SCR systems. Here, the filter and catalyst housing are used as a microwave resonant cavity as described in detail in previous publications by the authors [9,11,14,15]. Furthermore, similar resonance-based measurement approaches have also been investigated to monitor ammonia storage on SCR catalysts and

oxygen storage on three-way catalysts (TWC) using laboratory bench reactors [11,16].

Passive NOx SCR systems within the context of lean gasoline systems provide a unique opportunity for enhanced system control via RF sensing. Unlike the urea system, where continuous NH_3 supply is available from the urea tank, the passive SCR process explicitly relies on fuel-rich engine operation to generate ammonia over the TWC [17,18]. Ammonia formed over the TWC is subsequently stored on the downstream SCR catalyst and utilized for NOx reduction when the engine returns to lean operation. The challenge is to control the rich fueling events to meet ammonia generation demands, while at the same time,maintaining sufficient ammonia coverage on the SCR catalyst to reduce NOx emissions without consuming excessive amount of fuel, over all modes of transient operation.

The potential of the passive SCR approach to achieve high NOx conversion has previously been demonstrated over a pseudo-transient cycle representative of the conditions encountered during the Federal Test Procedure (FTP) drive cycle [19]. This work leverages the prior research and aims to exploit the potential opportunities of a closed-loop control of the engine fueling schedule using a feedback from the RF sensor to track the ammonia loading state of the SCR catalyst in real time. Testing, on a lean gasoline engine over a pseudo-FTP cycle was conducted in order to evaluate potential efficiency and performance gains enabled via more accurate ammonia inventory management using RF sensing.

PASSIVE SCR SYSTEM SETUP

The RF sensor used in this study was calibrated and deployed on a BMW N43B20 4-cylinder lean gasoline engine equipped with a passive SCR system. The engine was installed in a test cell at Oak Ridge National Laboratory and coupled to a motoring direct current dynamometer that controls the engine speed and load. The BMW lean gasoline engine utilized two lean combustion modes: lean stratified and lean homogenous. Lean stratified combustion is the leanest of the two with lambda ranging from 1.6 to 2.2, and it offers greater fuel-efficient benefits than lean homogeneous combustion. Up to 20% reduction in fuel consumption can be achieved with lean operation relative to stoichiometric; however, the engine only operates lean over a portion of the engine's speed and load range (up to 4500 rpm and 75% load). At higher engine speeds and loads, the engine operates in the stoichiometric combustion mode. The engine is also designed to operate in the stoichiometric mode over its entire operating range. In this study it was necessary to operate the engine fuel-rich for brief periods of time to generate the ammonia, and this was achieved by manual fuel injection adjustments to achieve the desired lambda. Additional information on the engine setup, performance and emissions can be found in previous publications [18-21].

To enable emissions and fuel economy measurements under realistic operating conditions, a pseudo-transient drive cycle described in [19] was employed. The cycle is a compilation of the six speed and load modal points with constant acceleration during speed and load changes. The modal points represent typical idle, acceleration and cruise events that the engine encounters during the FTP cycle.

The passive SCR system consisted of two TWCs followed by a GPF and a Cu-zeolite SCR. The front TWC was a 0.62 L palladium-based formulation without oxygen storage containing 7.33 g/L of palladium (Pd-TWC). This catalyst was obtained from the front half of the commercial dual zone TWC used in a 2009 PZEV (Partial Zero Emissions Vehicle) Chevrolet Malibu. A 0.82-L prototype TWC with NOx storage component (NSC) was installed downstream of the Pd-only TWC. The NS-TWC was provided by Umicore and contained platinum (Pt), palladium, rhodium (Rh) and oxygen and NOx storage materials with Pt/Pd/Rh loadings of 2.47/4.17/0.05 g/L. The combination of these TWC formulations were included in order to maximize NH_3 production while minimizing fuel consumptions associated with rich operation [22]. The Pd-TWC offers high NOx to NH_3 selectivity over a wide range of operating conditions, while the NS-TWC provides the benefits of extended lean operation as a result of lean NOx storage and increased NH_3 production from stored NOx during rich operation. Downstream of the TWC, a 2.47-L GPF followed by 2.47-L SCR were installed. The SCR catalyst is a small pore Cu-zeolite catalyst of a 400 cpsi substrate provided by Umicore. The TWCs were aged for 50 hours at 800 °C inlet temperature using stoich.-rich-lean aging protocol defined by the Advanced Combustion and Emission Control (ACEC) technical group [23]. The SCR was degreened in the engine exhaust for approximately 20 hours at 700 °C and had been exposed to the engine exhaust for approximately 100 hours with temperatures ranging between 200-500 °C as part of other studies. A schematic of the engine and after treatment is shown in Figure 3.

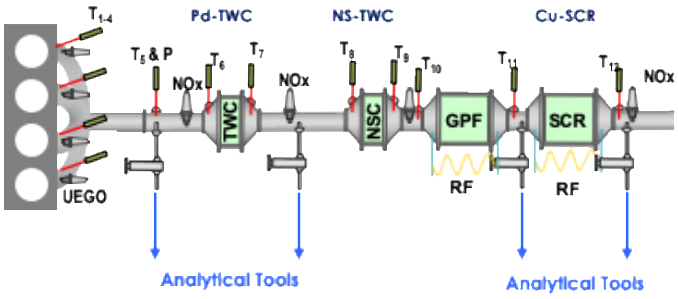

Figure 3. Engine and aftertreatment configuration. The RF sensor was placed over the SCR for ammonia inventory measurement.

RF SENSOR ON-ENGINE CALIBRATION

The RF sensor is designed to measure changes in the bulk dielectric properties within an enclosed cavity – in this case, the SCR. As ammonia is adsorbed on the catalyst surface, the bulk dielectric constant of the cavity material changes and the characteristics of the RF signal change. In this way, specific features of the RF spectrum are utilized to develop a transfer function which determines the ammonia loading state from these features and the measured substrate temperature. Prior to carrying out experiments with the passive SCR system, the RF sensor was first calibrated to the system.

Since the RF signal responds to both the ammonia adsorption on the catalyst and the temperature of the substrate, several ammonia adsorption/desorption isotherms were performed to calibrate the sensor. As these isotherms are performed at constant temperature, the RF spectral response to the ammonia adsorption alone may be characterized. An example of typical engine-out exhaust conditions is shown in Figure 4. Here the inlet and outlet ammonia and NOx sensor measurements are provided. During the adsorption portion of the isotherm, the inlet ammonia was held constant at 6 mg/s, and the inlet NOx was maintained at 0 mg/s. This condition was maintained even after initial ammonia breakthrough was observed, as during this time, the catalyst will still store additional ammonia even though the storage rate is reduced. Once the outlet ammonia trace reached steady state, it could be inferred that the system had reached equilibrium with the SCR fully saturated. Following a brief residence at this equilibrium state, the ammonia dosing was stopped.

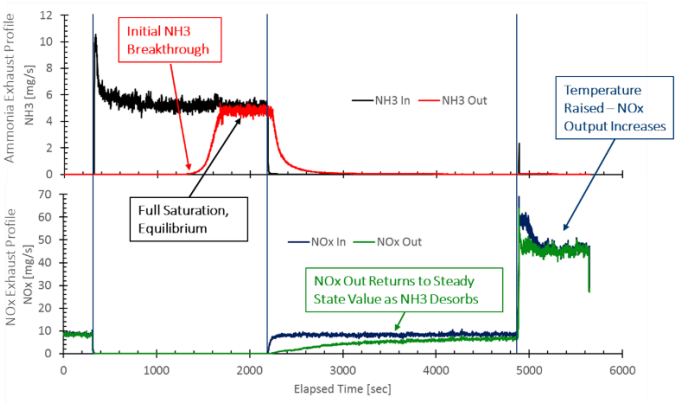

Figure 4. Engine-out exhaust conditions during a typical calibration isotherm.

In the second phase of the isotherm, NOx was introduced into the system to gradually consume the ammonia adsorbed on the catalyst. It can be seen that the outlet NOx measurements gradually return to the steady state value as the ammonia desorbed and was consumed. Finally, the temperature was raised and the NOx output increases. During this high-temperature portion of the test, any remaining ammonia was driven off the catalyst to return it to its empty state. This ammonia adsorption/desorption experiment was repeated at 25°C increments between 200 and 400°C.

The RF magnitude spectral response to ammonia adsorption, taken from scans obtained during the adsorption portion of the isotherm, is shown in Figure 5. The main resonances of the spectrum, as defined by the sharp peaks, are attenuated as ammonia is adsorbed on the catalyst. Depending on the temperature, the principal resonances may see 5-10 dB of attenuation in response to ammonia adsorption between the unloaded and the saturated state. Additionally, several of the troughs in the magnitude spectrum increase and become less sharp as ammonia is adsorbed on the catalyst. In developing a calibration, a relationship is established between the response of a selection of these features and the instantaneous ammonia load for each of the isotherm experiments.

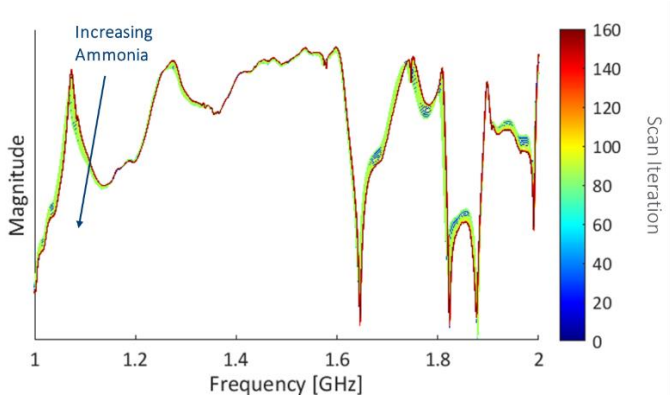

Figure 5. RF magnitude response to ammonia adsorption during a typical calibration isotherm.

After one or several spectral features are identified, a single parameter (RF statistic) is computed as the input to the transfer function. This RF statistic, along with the instantaneous ammonia storage inventory as measured from the test cell, is shown in Figure 6. In this figure, the ammonia storage inventory is shown to rise to the saturation point, just under 3 g/L. The RF statistic also rises during the adsorption portion of the isotherm test. During the desorption profile, both the inventory and RF statistic decrease. By matching the time series of ammonia inventory with the time series of the RF statistic, independent relationships between these two parameters may be established at each temperature.

These relationships are then combined into a three-dimensional representation of the transfer function. This representation is shown in Figure 7. Each row of points, shown by the blue dots, represents the relationship established between ammonia inventory and the RF parameter at that given temperature. Combined, a three-dimensional surface function is generated from the calibration data set.

The calibration shown in Figure 7 was loaded on the RF control module, and the ammonia load, as measured by the sensor, was sent via CAN and recorded by the test cell data acquisition system. This calibration and sensor communication configuration were utilized for the remainder of the experiments in this study.

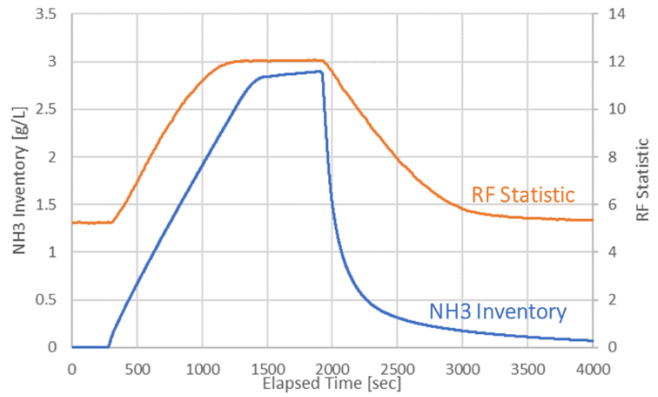

Figure 6. RF parameter response to ammonia adsorption at a nominal temperature of 250 °C.

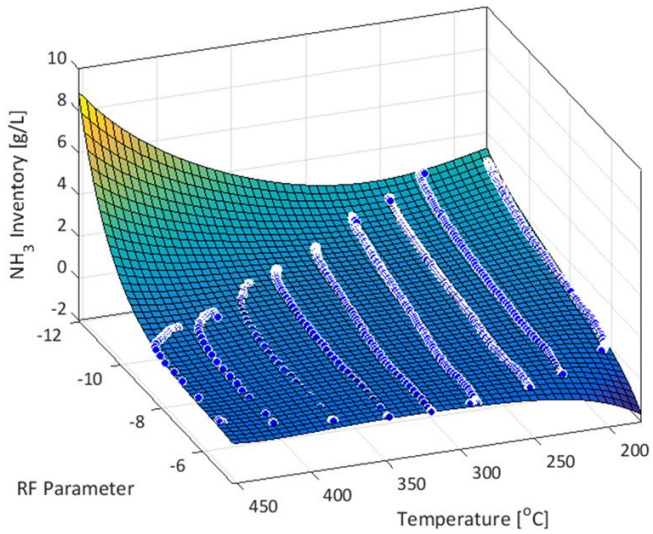

Figure 7. Calibration surface transfer function giving ammonia storage inventory as a function of RF and temperature.

RF SENSOR MEASUREMENT RESULTS

Figure 8 shows the impact of rich lambda conditions on the ammonia storage as measured by the RF sensor. A lambda value of 0.96 results in a large amount of ammonia generation, and therefore storage on the SCR, as shown by the green arrow in Figure 8(a), corresponding to an initial extended duration rich operation point. Further, spikes in the ammonia inventory are correlated with regions of rich operation during the FTP cycle, as indicated by the drops in lambda. During periods of lean operation, where lambda is greater than 1.0, ammonia stored on the catalyst is consumed by NOx in the exhaust stream. This can be seen in the RF measurements of ammonia inventory where regions of lean operation show a decrease in storage.

The sensitivity of lambda to the ammonia storage levels on the SCR are readily observed in the comparison between Figures 8(a) and (b). In the latter case, ammonia is generated in rich conditions where the lambda value is set higher at 0.99. In this case, less ammonia is generated under rich operation, particularly during the initial extended period of rich operation indicated by the green arrow. The spikes in the ammonia inventory signal are still correlated with periods of rich operation, as with the previous case, though smaller in magnitude due to the higher value of lambda. In this case, less stored ammonia is available for consumption during periods of lean operation. It can be seen from Figure 8(b) that towards the end of the FTP cycle, all the stored ammonia was depleted.

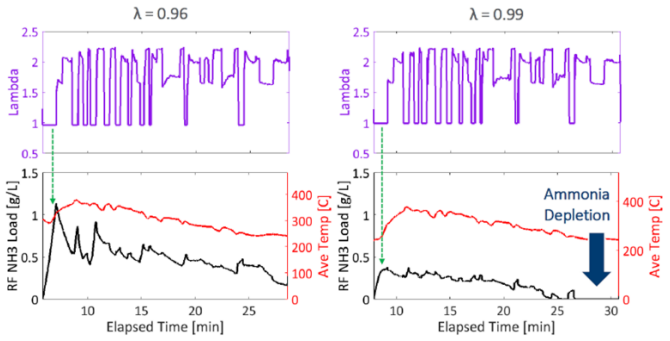

Figure 8. Air/fuel ratio, temperature and RF measured ammonia storage as a function of time for rich lambda of (a) 0.96 and (b) 0.99 during a single FTP cycle.

For the same two tests, the inlet and outlet NOx are compared to the RF measurements of ammonia storage in Figure 9. When lambda is lower during periods of rich operation, as in the case of the first FTP cycle shown in Figure 9(a), sufficient ammonia is stored on the catalyst to fully-convert nearly all the NOx during the cycle. Only during extended periods of high-NOx generation operation, such as near the end of the cycle at the 27-minute mark, does a trace amount of NOx slip through the catalyst.

In Figure 9(b), lambda during rich operation was set to 0.99. In this case, less ammonia was produced during rich operation, and therefore less was stored on the catalyst and available for NOx conversion during lean operation. In this case, the ammonia stored was fully depleted at the end of the cycle and results in significant NOx slip, as shown in the figure.

The results presented in Figures 8 and 9 assessed the RF sensor response to ammonia adsorption and NOx conversion at varying lambda. Ammonia inventory measurements demonstrated that reduced lambda during rich operation produced additional ammonia for storage on the catalyst, which

may be used for NOx conversion during lean engine operation. Several experiments were also run in order to determine NOx conversion efficiency improvements using a lean combustion strategy involving both lean stratified (LS) and lean Homogenous (LH) combustion. These modes are shown, with stoichiometric operation, on the engine speed and torque map in Figure 10.

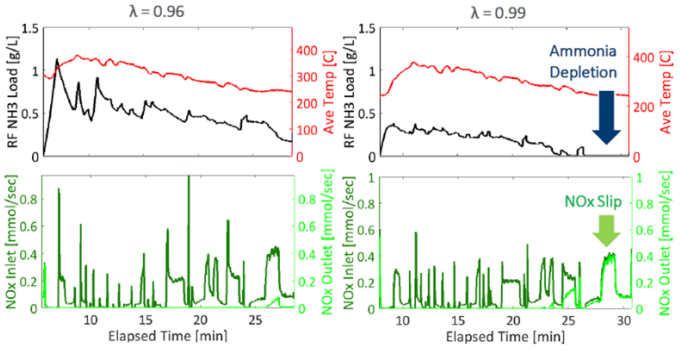

Figure 9. Time traces of temperature and RF measured ammonia storage, and inlet and outlet NOx showing NOx slip for lambda of (a) 0.96 and (b) 0.99 during a single FTP cycle.

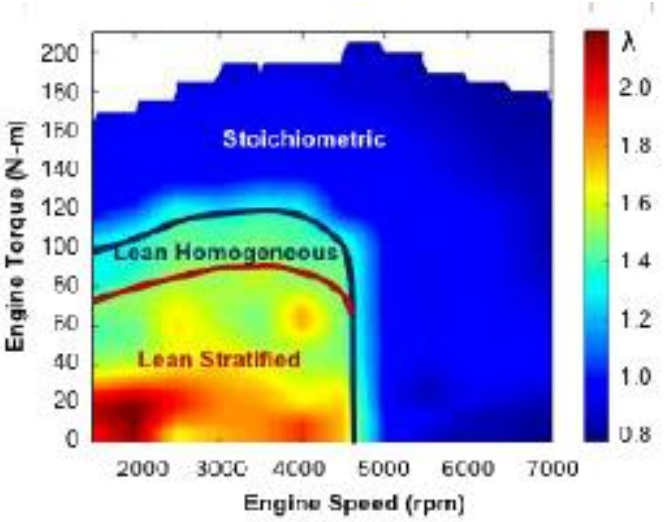

Figure 10. Engine speed and torque map for the BMW N43B20 lean gasoline engine showing stoichiometric, lean homogenous and lean stratified modes.

Figure 11 presents the first lean combustion strategy that was developed and evaluated over the course of repeated 6-mode pseudo-transient FTP cycles. This strategy utilized both lean homogenous and lean stratified operation to increase engine efficiency. In this strategy as shown in Figure 11, the FTP is initialized with a period of rich operation at lambda of 0.99 to both generate ammonia and simulate an actual cold start case. Following this startup period, the engine was defaulted to run in lean operation. The ECU used was open access and allowed for customization of the engine run conditions. The lean homogenous and lean stratified operation conditions were not prescribed, however are indicated by the open and outlined green symbols, respectively. For the rest of the cycle, if the NOx concentration at the SCR inlet exceeded 20 ppm, rich operation was commanded. Lambda was then set to 0.98 for the remainder of the cycle during rich operation.

The input-output response under the first lean combustion strategy with lambda of 0.98-0.99 is shown in Figure 12. As with previous experiments, the ammonia inventory as measured by the RF sensor is well correlated with the system input as given by lambda. During periods of rich operation, where lambda is less than 1.00, and where ammonia is generated, the ammonia inventory increases. This can be seen from Figure 12 where the green arrows indicate regions of extended rich operation. Additionally, ammonia is consumed from the catalyst during periods of lean operation where lambda increases above 1.00.

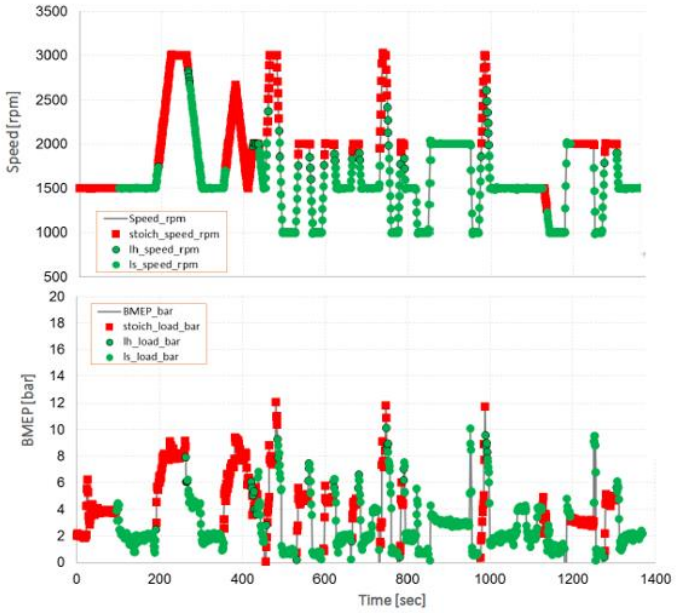

Figure 11. First lean combustion strategy – lean to rich cycling with both lean stratified (LS) and lean homogenous (LH) operation with hard acceleration at lambda = 0.995.

It has been shown that the input-output response, as given by lambda, which is an indication of ammonia generation and consumption, and the instantaneous ammonia inventory measured by the RF sensor, are well correlated. Figure 13 shows the gaseous emissions measurements upstream and downstream of the catalyst along with the RF measurements of ammonia inventory and demonstrates that the inventory is well-correlated with these emissions measurements as well. During periods of ammonia generation, indicated by large values of inlet ammonia concentration, the ammonia inventory of the catalyst increases. This indicates that ammonia generated during rich operation is stored on the catalyst and available for NOx conversion. During the second and third FTP cycle, it can be seen that some ammonia is slipped at the middle of the cycle. This accounts for

an average of 26.5% of the overall ammonia per cycle, integrated over the whole cycle and occurs at periods of high temperature, where the storage capacity of the catalyst is reduced.

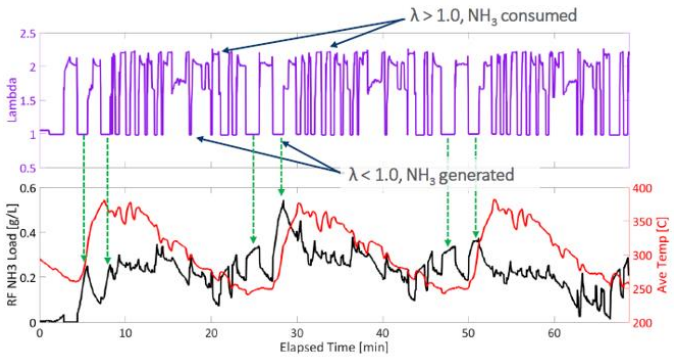

Figure 12. Input-output response of the first multimode strategy with lean homogenous combustion.

Figure 13 also shows that the ammonia inventory as measured by the RF sensor is well-correlated with NOx concentration in the exhaust. Large bursts in engine-out NOx result in a reduction of the overall ammonia storage measurement as indicated by the RF sensor. During the last FTP cycle, trace amounts of NOx are measured in the tailpipe. Over the entire FTP cycle, the system is able to achieve 99.5% NOx conversion. Overall, this combustion strategy is able to provide a 7.6% improvement in fuel economy, and further feedback optimization using the RF sensor for ammonia inventory may provide improved conversion with less ammonia slip.

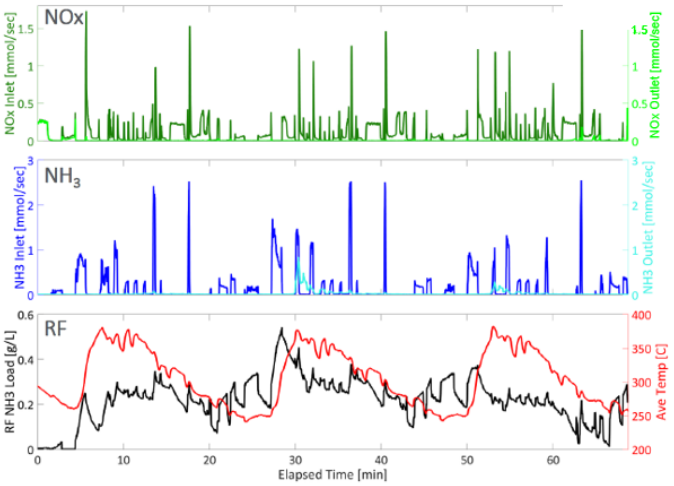

Figure 13. NOx conversion and ammonia storage during the first multimode strategy with lean homogenous combustion.

A second lean combustion strategy was developed and utilized for the course of an FTP cycle and is shown in Figure 14. This strategy used a combination of lean homogenous and lean stratified operation to increase engine efficiency. As with the first strategy as shown in Figure 11, the FTP sequence is initialized with a period of rich operation at lambda of 0.99. The first hard acceleration was run at a lambda of 0.995. Following this startup period, the engine was run in lean operation as the default setting. The open and outlined symbols in Figure 14 indicate lean homogenous and lean stratified operation, respectively. For the remainder of the cycle, rich operation was commanded to lambda of 0.98 only if the NOx at the SCR inlet exceeded 20ppm.

Again, the input-output response for the second lean combustion strategy is shown in Figure 15. The ammonia inventory, which is measured by the RF sensor, is well correlated with the system input as given by lambda. During periods of rich operation, where lambda is less than 1.00, and where ammonia is generated, the ammonia inventory responds and increases. In this case, the increase in ammonia storage is much less than in previous cases. Additionally, where lambda increases above 1.00 during periods of lean operation, ammonia is consumed from the catalyst. The calibrated RF sensor output shows this behavior in the bottom plot of Figure 15.

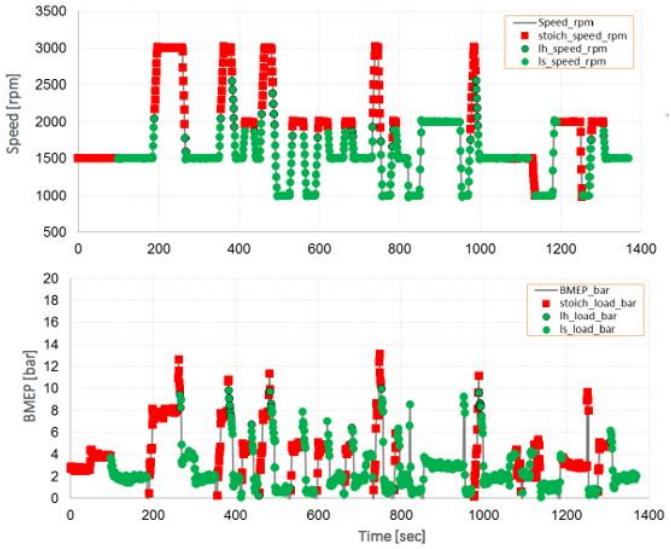

Figure 14. Second lean combustion strategy – lean to rich cycling with both lean stratified (LS) and lean homogenous (LH) operation.

During the second multimode combustion strategy with lean homogenous and lean stratified combustion, the gaseous emissions are again well-correlated with the RF-measured ammonia inventory as shown in Figure 16. The ammonia dosing strategy is consistent with previous FTP cycles, however due to the engine management strategy the ammonia inventory is maintained at a significantly lower level. While periods of high inlet ammonia concentrations result in increased ammonia storage, these increases are significantly reduced from the first control strategy. With this engine management strategy, the amount of ammonia slipped is greatly reduced to only 3.2% over

the FTP cycle. The spike in stored ammonia at the end of the cycle results from the high temperatures required to regenerate the catalyst. The sensor is not calibrated at these temperatures and is extrapolating values in this regime. Additional experiments could be performed to calibrate the sensor at these temperatures, but with diminishing returns as the catalytic coating is not capable of storing ammonia under these conditions.

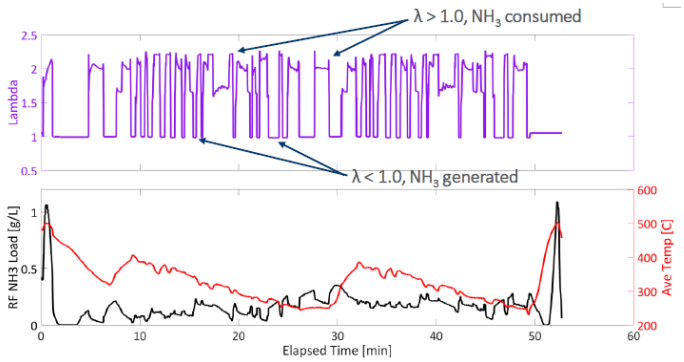

Figure 15. Input-output response of the second multimode strategy with lean homogenous combustion.

Figure 16 also shows that the ammonia inventory measurement is well-correlated with NOx concentration in the exhaust. Large bursts in engine-out NOx result in a reduction of the overall ammonia storage measurement as provided by the RF sensor. Minimal NOx is measured in the tailpipe, with an overall conversion efficiency of 98.0%. Additionally, this engine management strategy is able to provide a 9.3% improvement in fuel economy over the entire FTP cycle. Instantaneous measurements of ammonia inventory, as provided by the RF sensor, provides an integral feedback component required to implement such a strategy.

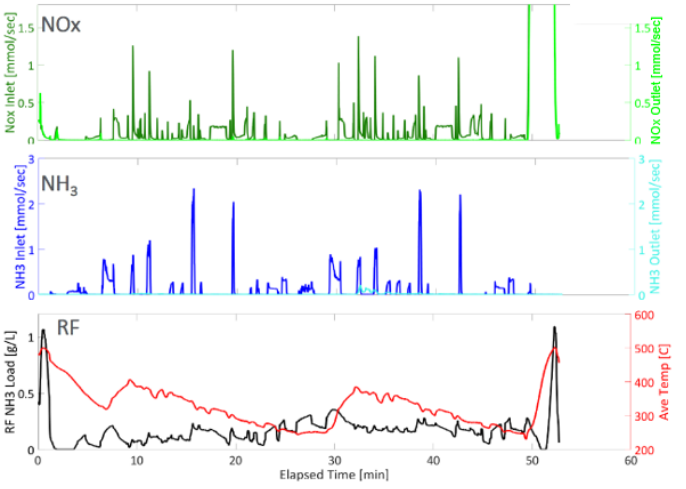

Figure 16. NOx conversion and ammonia storage during the second multimode strategy with lean homogenous combustion and without hard acceleration.

CONCLUSION

This study evaluated various lean combustion strategies in combination with a passive SCR system and RF sensor capable of directly monitoring catalyst ammonia storage levels. The results demonstrated that utilizing a combination of lean stratified and lean homogenous operation was able to provide improvements in both fuel economy NOx conversion, by up to 9.3% (relative to stoichiometric) and 99.5%, respectively. Furthermore, optimization of rich-lean cycling between lean stratified and lean homogenous operation, reduced ammonia slip by over 20%.

The RF sensor was calibrated while on-engine via a series of ammonia adsorption-desorption isotherm profiles. Direct measurements of ammonia inventory on the SCR were achieved via the use of the calibrated RF sensor, which proved to be well-correlated with both estimates of catalyst ammonia storage and exhaust gas measurements. Experiments in the study were all performed open-loop with a predefined engine control and ammonia generation strategy via rich operation in order to evaluate the RF sensor response. Future work will focus on closed-loop control using feedback from the RF sensor to optimize the catalyst inventory. Such implementation would allow for finer control of the ammonia dosing strategy. It would also provide direction for combustion mode switching of the engine to reduce ammonia slip and optimize NOx conversion.

ACKNOWLEDGEMENTS

This material is based upon work supported by the Department of Energy under contract DE-EE0007214. The authors would like to thank Roland Gravel from the DOE and Jason Conley from DOE NETL for their support and engaging discussions. The authors would also like to thank the support from Commercial and National Laboratory Project Partners: Corning Incorporated, Oak Ridge National Laboratory, Daimler Trucks NA / Detroit Diesel, Cummins, FCA and DSNY.

REFERENCES

1. Official Journal of the European Union, "Regulation (EC) No. 715/2007 of the European Parliament and of the council of 20 June 2007," 2007.
2. California Air Resources Board, "Proposed Greenhouse Gas (GHG) Regulations for Medium- and Heavy-Duty Engines and Vehicles, Optional Reduced Emission Standards for Heavy-Duty Engines," Staff Report, ARB, California, 2013.
3. Majewski, W. A. (2015), "SCR Systems for Mobile Engines," DieselNet.com, Retrieved May 02, 2016, from https://www-dieselnet.com.libproxy.mit.edu:9443/tech/cat_scr_mobile.php, Copyright © EcopointInc. Revision 2005.05e)
4. Cavataio, G., Girard, J., and Lambert, C., "Cu/Zeolite SCR on High Porosity Filters: Laboratory and Engine Performance Evaluations," SAE Technical Paper 2009-01-0897, 2009.
5. Hannu Jääskeläinen, Majewski, W. A. (2015), "Urea Dosing Control," DieselNet.com, Retrieved May 02, 2016, from http://www.dieselnet.com.libproxy.mit.edu/tech/cat_scr.php Copyright © EcopointInc. Revision 2015.10)
6. Majewski, W. A. (2015), "Urea Dosing and Injection Systems" DieselNet.com, Retrieved May 02, 2016, from http://www.dieselnet.com.libproxy.mit.edu/tech/cat_scr.php , Copyright © EcopointInc. Revision 2015.10)
7. Majewski, W. A. (2015), "Selective Catalytic Reduction," DieselNet.com, Retrieved May 02, 2016, from http://www.dieselnet.com.libproxy.mit.edu/tech/cat_scr.php , Copyright © EcopointInc. Revision 2015.10)
8. Kleemann, M., Elsener, M., Koebel, M., and Wokaun, A., "Hydrolysis of Isocyanic Acid on SCR Catalysts," Ind. Eng. Chem. Res. 39(11):4120-4126, 2000, doi:10.1021/ie9906161.
9. Ragaller, P., Sappok, A and Bromberg, L., "Particulate Filter Soot Load Measurements using Radio Frequency Sensors and Potential for Improved Filter Management," SAE Technical Paper 2016-01-0943, 2016.
10. Nanjundaswamy, H., Nagaraju, V., Wu, Y., Koehler, E., Sappok, A., Ragaller, P., and Bromberg, L., "Advanced RF Particulate Filter Sensing and Controls for Efficient Aftertreatment Management and Reduced Fuel Consumption," SAE Technical Paper 2015-01-0996, 2015.
11. Moos, R., "Microwave-Based Catalyst State Diagnostics – State of the Art and Future Perspectives," SAE International Journal of Engines, Vol. 8, No. 3, 2015.
12. Sappok, A., Bromberg, L., Parks, J., and Prikhodko, V., "Loading and Regeneration Analysis of a Diesel Particulate Filter with a Radio Frequency-Based Sensor," SAE Technical Paper 2010-01-2026, 2010, doi: 10.4271/2010-01-2126.
13. Sappok, A. and Bromberg, L., "Radio Frequency Diesel Particulate Filter Soot and Ash Level Sensors: Enabling Adaptive Controls for Heavy-Duty Diesel Applications," SAE Int. J. Commer. Veh. 7(2):468-577, 2014, doi: 10.4271/2014-01-2349.
14. Sappok, A., Ragaller, P., Bromberg, L., Prikhodko, V., Storey, J., and Parks, J., "Real-Time Engine and Aftertreatment System Control Using Fast Response Particulate Filter Sensors," SAE Technical Paper 2016-01-0918, 2016.
15. Sappok, A., Ragaller, P., Bromberg, L., Herman, A., Prikhodko, V., Parks, J., and Storey, J., "On-Board Particulate Filter Failure Prevention and Failure Diagnostics using Radio Frequency Sensing," *SAE International Journal of Engines*, Vol. 10, No. 4, 2017.
16. Rauch, D., Kubinski, D., Cavataio, G., Upadhyay, D. et al., "Ammonia Loading Detection of Zeolite SCR Catalysts using a Radio Frequency based Method," *SAE International Journal of Engines*, Vol. 8, No. 3, 2015.
17. W. Li, K. L. Perry, K. Narayanaswamy, C. H. Kim, and P. Najt, "Passive Ammonia SCR System for Lean-burn SIDI Engines," *SAE Int. J. Fuels Lubr.*, vol. 3, no. 1, pp. 2010-01–0366, Apr. 2010.
18. V. Y. Prikhodko, J. E. Parks, J. A. Pihl, and T. J. Toops, "Ammonia Generation and Utilization in a Passive SCR (TWC+SCR) System on Lean Gasoline Engine," *SAE Int. J. Engines*, vol. 9, no. 2, pp. 2016-01–0934, Apr. 2016.
19. Prikhodko, V.Y., Pihl, J.A., Toops, T.J. et al., "Passive SCR performance under pseudo-transient cycle: challenges and opportunities for meeting Tier 3 emissions," *Emission Control Science and Technology (2019)*. https://doi.org/10.1007/s40825-019-00126-1
20. P. Chambon, S. Huff, K. Norman, K. D. D. Edwards, J. Thomas, and V. Y. Prikhodko, "European Lean Gasoline Direct Injection Vehicle Benchmark," in *SAE Technical Paper 2011-01-1218*, 2011.
21. V. Y. Prikhodko, J. E. Parks, J. A. Pihl, and T. J. Toops, "Passive SCR for lean gasoline NOX control: Engine-based strategies to minimize fuel penalty associated with catalytic NH3 generation," *Catal. Today*, vol. 267, pp. 202–209, Feb. 2016.
22. V. Prikhodko, J. Pihl, T. Toops, and J. Parks, "Effects of NOx Storage Component on Ammonia Formation in TWC for Passive SCR NOx Control in Lean Gasoline Engines," SAE Technical Paper 2018-01-0946, 2018.
23. "Aftertreatment Protocols for Catalyst Characterization and Performance Evaluation: Low-Temperature Oxidation Catalyst Test Protocol", April 2015. Accessed on May 5, 2019 at https://cleers.org/wp-content/uploads/2015_LTAT-Oxidation-Catalyst-Characterization-Protocol.pdf